



Photosynthetic efficiency and nutrient physiology of the diatom *Thalassiosira pseudonana* at three growth temperatures

Samantha J. Gleich^{1,2} · Louis V. Plough¹ · Patricia M. Glibert¹

Received: 6 February 2020 / Accepted: 9 July 2020 / Published online: 5 August 2020
© Springer-Verlag GmbH Germany, part of Springer Nature 2020

Abstract

Diatom cells utilize a variety of metabolic pathways to cope with internal energy imbalances caused by stressful environmental conditions. In this study, the model diatom species, *Thalassiosira pseudonana*, was grown in nutrient replete and nitrate (NO_3^-)- and dissolved silicate (Si)-depleted media at three growth temperatures (4, 17, 28 °C) to determine how nutrient enrichment and temperature affects diatom growth, photosynthetic efficiency, nitrate reductase (NR) enzyme activity, biogenic silica (bSiO_2) deposition, and NR gene expression. Growth rates for nutrient-replete cultures were highest at 17 °C. Across all nutrient treatments, the cells grown at 17 °C had an average Fv/Fm of 0.44 ± 0.006 , while the cells were grown at 4 °C and 28 °C had an average Fv/Fm of 0.37 ± 0.004 and 0.38 ± 0.01 , respectively. Activity of NR was variable across treatments with no significant effect of temperature. The relative expression of the targeted NR gene was, on average, ~10 times higher in the 4 °C cultures and ~4 times higher in the 28 °C than in the 17 °C cultures, while the activity of the NR enzyme was generally highest in the cultures grown at 17 °C that were enriched with NO_3^- . Cells grown under nutrient-replete conditions had significantly higher bSiO_2 deposition rates at 4 °C than cells grown at 17 and 28 °C. These data support the notion that cold, nutrient-replete conditions lead to increases in diatom silicification and that NR activity may be regulated downstream of mRNA transcription under specific environmental conditions.

Introduction

Diatoms make substantial contributions to new production in marine and freshwater ecosystems and have been estimated to fix over 10 billion tons of inorganic carbon (C) in the oceans each year (Goldman 1993; Del Amo et al. 1997; Brzezinski et al. 1998; Smetacek 1998; Granum et al. 2005). In addition to the significant role that diatoms play in global primary production, these organisms are also important in the export of C from the euphotic zone and in the biogeochemical cycling of nutrients in aquatic ecosystems (Round

et al. 1990; Raven and Falkowski 1999; Ragueneau et al. 2006). Although diatoms are widely distributed and appear to be “cosmopolitan” in nature (Finlay and Fenchel 2004), they do have environmental preferences and changes in the surrounding environment can stress them and impact their growth and productivity.

Diatoms often dominate phytoplankton assemblages during the onset of spring blooms and in upwelling regions when waters are cool, nutrient-rich, and weakly stratified (Cushing 1989; Peinert et al. 1989; Eppley et al. 1969b; Lomas and Glibert 1999a). Following spring freshets and upwelling events, waters that are injected into the euphotic zone are typically rich in nitrate (NO_3^-) and dissolved silicate (Si), both of which may help fuel diatom blooms. The availability of oxidized NO_3^- relative to chemically-reduced nitrogen (N) forms (e.g., ammonium, NH_4^+), can also play an important role in diatom growth and productivity because diatoms often prefer NO_3^- over NH_4^+ (Probyn and Painting 1985; Lomas and Glibert 1999a; Glibert et al. 2016). Given that Si is necessary for diatom cells to divide, and the general preference for NO_3^- by diatoms, the relative availability of Si and NO_3^- may influence diatom abundance.

Responsible Editor: S. Shumway.

Reviewed by undisclosed experts.

✉ Patricia M. Glibert
glibert@umces.edu

¹ Horn Point Laboratory, University of Maryland Center for Environmental Science, P.O. Box 775, Cambridge, MD 21613, USA

² Present Address: Department of Biological Sciences, University of Southern California, 3616 Trousdale Parkway, AHF 301, Los Angeles, CA 90089-0371, USA

However, even when essential nutrients are readily available in the water column, other environmental factors such as water temperature may affect diatom growth and productivity. Water temperature becomes an important controlling variable when the pathways of N and C assimilation become uncoupled. Typically, the light-dependent reactions of photosynthesis are unaffected by temperature, while the Calvin cycle, responsible for C assimilation, slows down as temperatures decrease (Kok 1956; Falkowski and Raven 1997). The Calvin cycle enzyme Rubisco is responsible for the first step of C fixation and typically has a temperature optimum of ~ 30 °C or greater (Li 1980; Smith and Platt 1985; Ras et al. 2013). In contrast, the NO_3^- reductase (NR) enzyme that is responsible for catalyzing the reduction of NO_3^- to nitrite (NO_2^-) has been found to operate optimally when temperatures are cool (~ 10 – 20 °C; Lomas and Glibert 1999a; Gao et al. 2000; Berges et al. 2002). If Rubisco activity declines as temperatures decrease, excess reductant may build up from the biophysical light reactions which can lead to photodamage or photoinhibition (Falkowski and Raven 1997; Sobrino and Neale 2007; Glibert et al. 2016). To overcome this imbalance, diatoms have been shown to reduce NO_3^- to NO_2^- and then to NH_4^+ in a non-assimilatory fashion (Lomas and Glibert 1999a, b; Glibert et al. 2016) thus making dissimilatory NO_3^- reduction an efficient energy dissipation, ‘overflow’, pathway when temperatures are cool and the NR enzyme is operating efficiently. However, at temperatures well below ~ 10 °C or well above ~ 20 °C, the efficiency of dissimilatory NO_3^- reduction may decrease. At high temperatures, the coupling between N assimilation and Rubisco activity increases, reducing the need for this overflow pathway, whereas at very low temperatures, the activity of NR decreases (Kristiansen 1983; Berges et al. 2002). Therefore, overflow pathways other than dissimilatory NO_3^- reduction may be necessary for diatom cells to overcome internal energy imbalances that occur when photochemistry and C fixation become uncoupled at temperatures less than those that are optimal for NR. Photorespiration is one such pathway (Huner et al. 1998; Parker and Armbrust 2005; Glibert et al. 2016). As a whole, photorespiration is an energetically inefficient process that results in a net loss of C fixation; however, increases in photorespiration may work to alleviate the stress that diatoms experience when photochemistry and C fixation become uncoupled (Parker and Armbrust 2005; Glibert et al. 2016).

It has been suggested that increases in photorespiration may stimulate mitochondrial urea cycle activity that is, in turn, related to the synthesis of polyamines in diatom cells (Liu and Glibert 2018). These polyamines are incorporated into the silaffin proteins that are involved with biogenic silica (bSiO_2) deposition in diatom cell walls (Sumper and Kröger 2004; Nunn et al. 2013; Hildebrand et al. 2018). Therefore, if increases in photorespiration stimulate urea cycle activity

and lead to increases in polyamine synthesis, silicification may increase (Liu and Glibert 2018). Heavily silicified diatoms have a greater propensity for sinking, which may lead to increased bSiO_2 export from the photic zone (e.g., Dugdale et al. 1995). Thus, the degree of silicification can affect the rates of dissolution and biogeochemical cycling of bSiO_2 , altering the subsequent availability of Si to diatoms in the water column (Liu and Glibert 2018).

The goal of this study was to use the model diatom species, *Thalassiosira pseudonana*, to quantify the relationships between nutrient availability, photosynthesis, NR enzyme activity, silicification, and NR gene expression when cells were growing at three temperatures: at or near the presumed NR temperature optima (17 °C), well above it and near the optimal temperature for Rubisco (28 °C), and well below the optimal temperature of both enzymes (4 °C). It was hypothesized that diatom fluorescence characteristics, NR enzyme activity, and NR gene expression should increase when temperatures are near the NR temperature optima and when NO_3^- and Si are not limiting. In contrast, cold, nutrient-replete conditions should increase photochemical stress in diatom cells and should lead to decreases in NR activity and gene expression and increases in cell wall silicification. The information obtained through this study may begin to elucidate how metabolic energy balance and overflow pathways function in this diatom species under different temperature and nutrient conditions.

Materials and methods

Culture conditions and experimental design

A stock culture of *T. pseudonana* CCMP 1335 was obtained from the Horn Point Laboratory Oyster Hatchery. It was transferred to *f/2* culture media, made with filtered seawater (Guillard 1983) and acclimated to three temperatures, 4 °C, 17 °C, and 28 °C, over the course of several weeks to months (Fig. 1). Multiple substock cultures were maintained at these temperatures in batch conditions under a 12:12 light:dark cycle at a light level of $\sim 200 \mu\text{E m}^{-2} \text{s}^{-1}$, gently bubbled with CO_2 . The growth rates of replicated substocks were measured after the acclimation period as described below.

When the temperature-acclimated cultures were in the exponential phase of growth, cells were concentrated by filtration or centrifugation and were transferred into 2-liter culture flasks that contained NO_3^- and Si-depleted media and held at the same environmental conditions as the substock cultures (Fig. 1). Nutrient-depleted media was made by adding all *f/2* nutrients except for NO_3^- and Si to filtered seawater. Cell growth in the nutrient-depleted cultures was monitored until the cells in these nutrient-depleted cultures

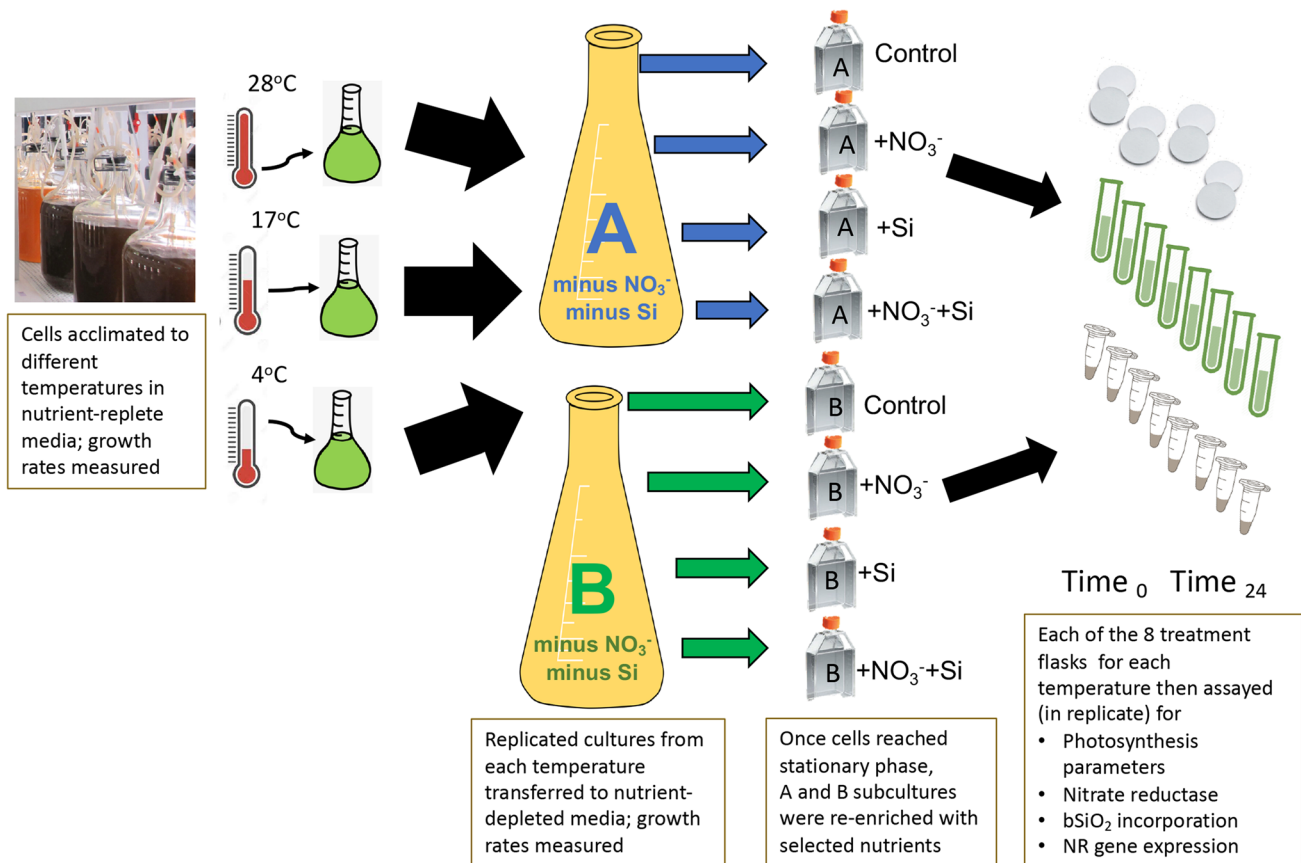


Fig. 1 Flow diagram of the experimental design. Replicated temperature-acclimated cultures, derived from a single stock culture, were transferred to nutrient-depleted media, then enriched with selected nutrients and individually assayed for various physiological param-

eters. The treatment additions of NO₃⁻ and Si were 100 μM. In all, 4 fully-replicated treatment conditions were assayed at 3 temperatures at two-time points. See text for method details

reached stationary phase (residual nutrient permitted short-term growth).

On the first day that a decline in growth rate was noted, 500 mL of each nutrient-depleted culture were transferred into 4 separate polyethylene culture flasks, which were then enriched with 3 different combinations of nutrients (Fig. 1), yielding a fully-replicated suite of treatments for each temperature. Additions of either NO₃⁻ and/or Si were made at 100 μM. Control flasks received no added nutrients.

Immediately after making the nutrient additions, and again 24 h later, aliquots were removed from the treatment flasks for measurements of cell abundance, concentrations of NO₃⁻ and Si, variable fluorescence characteristics, NR enzyme activity, bSiO₂ deposition, and the relative expression of a gene that is associated with NR activity (Fig. 1).

Cell abundance quantification

To quantify cell abundance in each of the experimental containers, 1.5 mL of each culture were fixed with 10% paraformaldehyde and stored at 4 °C until analysis. Cell counts

were then obtained using a BD Accuri C6 flow cytometer with dual excitation (488 nm, 640 nm). When analyzed on the flow cytometer, cells were gated by shape and size using forward scatter and side scatter settings. Cell concentrations were calculated by dividing absolute cell counts by the volume of the sample that was analyzed.

Nutrient analyses

Aliquots of media from all flasks were filtered through pre-combusted GF/F filters, and the filtrate was frozen at -18 °C until nutrient analyses were performed. Concentrations of NO₃⁻ were determined to replicate according to Miranda et al. (2001) and Doane and Horwath (2003). Concentrations of Si were determined at Horn Point Analytical Services Laboratory according to Zimmerman et al. (1977).

PAM fluorometry

Variable fluorescence parameters were obtained using a Walz Phyto-PAM II fluorometer. At each sampling time,

duplicate 2 mL of each culture treatment were collected and placed in a glass test tube. The samples were then placed in darkness for 15–20 min. After the dark incubation period, the algal quantum efficiency (F_v/F_m) and maximum electron transport rate (ETR_{max}) were measured. The ETR_{max} values were calculated according to Genty et al. (1989).

Nitrate reductase activity

Activity of NR was measured using the NO_3^- reduction protocol of Eppley et al. (1969a) as modified by Berges and Harrison (1995). For each treatment, two aliquots of 25 mL were each filtered onto a precombusted GF/F filter, then flash frozen and stored at $-80^\circ C$ until analysis. After no more than 1 week, the frozen GF/F filters were homogenized in a glass Teflon homogenizer with 3.3 mL of extraction buffer. The extraction buffer contained 1 mM of dithiothreitol, 5 mM EDTA, 0.2 M phosphate buffer, 0.1% v/v Triton X-100, and 0.3% w/v polyvinyl pyrrolidone, and was adjusted to a pH of ~ 8 using potassium hydroxide pellets. The homogenized filter material was centrifuged for 5 min at $4^\circ C$ and $1744\times g$. Then, the supernatant of each replicate was divided into two, 1 mL portions, one of which was used as a control and one was used for the NO_3^- reduction reaction. The control and reaction tubes were all incubated at their respective experimental growth temperatures (4 , 17 , or $28^\circ C$) for 30 min. The control tubes were incubated with 0.2 M $NaNO_3^-$, 0.05 M $MgSO_4^-$, and 300 μL extraction buffer, and the treatment tubes were incubated with 0.2 M $NaNO_3^-$, 0.05 M $MgSO_4^-$, and 300 μL of 150 μM NADH. The reactions were stopped by adding 1 M zinc acetate and 5 mL of 95% ethanol. The samples were then centrifuged for 5 min at $15^\circ C$ and $1744 \times g$. Excess NADH was oxidized by adding 0.83 μM phenazine methosulfate to the supernatant obtained by centrifugation. Then, the supernatant was used to determine NO_2^- formation in each of the samples, quantified spectrophotometrically (Eppley et al. 1969a; Parsons et al. 1984). To determine NO_2^- concentrations in each of the samples, 800 μL of supernatant was combined with 32 μL of the color detection reagent. Following color development, absorbance readings were measured at 543 nm on a BioTek Synergy HT or a BioTek Synergy LX plate reader. The NR activity values were normalized to cell abundance to determine NR activity $cell^{-1} h^{-1}$ and results of the replicate filters averaged.

Silica deposition rate

For measurements of silicification, the fluorescent analog, 2-(4-pyridyl)-5-((4-(2-dimethylaminoethylaminocarbonyl)methoxy)phenyl)oxazole (PDMPO), was used. This compound is incorporated into diatom cell walls at a constant ratio with $bSiO_2$ (Shimizu et al. 2001; McNair et al. 2015).

Subsamples were collected from each treatment flask, placed in small polyethylene bottles and inoculated with PDMPO to yield a final concentration of 0.157 μM . This concentration of PDMPO was based on preliminary analyses that showed that this concentration was sufficient to saturate incorporation overtime at the culture conditions used during the experiment. The bottles were incubated at the temperature of culture growth (4 , 17 , or $28^\circ C$) for 24 h and samples were subsequently analyzed according to McNair et al. (2015) and Shimizu et al. (2001). First, the cells in each bottle were filtered in replicate onto a 14 mm polycarbonate filter which was placed in a 15 mL polyethylene tube, covered with 10 mL 100% methanol, and placed in the dark at $4^\circ C$ for 24 h. Following the 24-h incubation, the filters were compressed at the bottom of the tube using a Teflon rod and the tubes were centrifuged for 10 min at $1211\times g$. Then, 9 mL of the methanol were removed from each tube and the tubes were left to dry (uncapped) in a $50^\circ C$ oven. Once the filters were dry, 200 μL of 0.5 M hydrofluoric acid (HF) were added to each tube and the tube was mixed using a Teflon rod. The tubes with HF were incubated for 3 h and 2.8 mL of 1 M boric acid were added to each of the tubes. Finally, 2 mL were transferred from these tubes into a cuvette with 1 mL of 100% methanol. Fluorescence measurements were obtained using a FluoroMax fluorometer (excitation: 365/30, emission: 534/30) and were compared to a standard curve consisting of PDMPO in a matrix of HF and boric acid. The concentration of $bSiO_2$ deposited into the culture cells was estimated using a $bSiO_2$:PDMPO ratio of 2900:1 when the silicic acid ($Si(OH)_4$) concentration was greater than 3 μM and using the equation $bSiO_2$:PDMPO = $912.6 * [Si(OH)_4]$ when the concentration of $Si(OH)_4$ was less than 3 μM (McNair et al. 2015).

Gene expression analysis

A NR gene (*NR*) was targeted for differential gene expression analysis. Primers used to target *NR* were obtained from Parker and Armbrust (2005); (Table 1). To quantify differential expression, actin (*Actin*) was used as a housekeeping gene, and those primers were obtained from McGinn and Morel (2008). The PCR products that resulted from the differential expression analyses were run on a 1% agarose gel to confirm that the primers used were specific and that the target sequences were properly amplified. Additionally, PCR reaction efficiencies were calculated according to Wacker and Godard (2005).

To extract total RNA, ~ 50 mL of culture were filtered onto a Supor-200 membrane filter. Cells captured on the filter were scraped into a clean microcentrifuge tube, lysed using a pestle, and flash frozen in liquid N_2 . Total RNA from the cells was extracted using the Qiagen RNeasy Plant Mini Kit. The total RNA that was obtained from each RNA

Table 1 PCR primer sequences used in this study

Target gene	Primer sequence	Fragment size (bp)	References
Actin (<i>Actin</i>)	F: ACTGGATTGGAGATGGATGG R: CAAAGCCGTAATCTCCTTCG	162	Parker and Armbrust (2005)
Nitrate reductase (<i>NR</i>)	F: TGAGGAAGCATAACAAGGAGG R: AGCATCAGAAACAACCGCCA	233	McGinn and Morel (2008)

extraction was incubated with Invitrogen DNase I to ensure that genomic DNA was not a source of contamination in the subsequent analyses. Following the RNA extraction and DNA digestion protocols, total RNA was quantified using a Qubit RNA HS Assay Kit. The total RNA obtained from each culture was stored at $-80\text{ }^{\circ}\text{C}$ until RT-qPCR procedures were performed. All of the RT-qPCR procedures were carried out within 2 weeks of the RNA extraction protocol.

Following RNA quantification, the RT-qPCR analyses were conducted using the QIAGEN one-step QuantiNova SYBR Green RT-PCR Kit. To run the RT-qPCR analysis, 5 μL of total RNA were added to a mixture containing 10 μL 2 \times SYBR Green RT-PCR Master Mix, 0.2 μL QN SYBR Green RT-Mix, 1 μL of both the forward and reverse primers (10 μM), and 2.8 μL of RNase-free water, for a total reaction volume of 20 μL . The reaction mixtures were then run on a Bio-Rad CFX96 qPCR machine using the Bio-Rad CFX Manager software. The first reverse transcription step of the reaction was $50\text{ }^{\circ}\text{C}$ for 10 min. Following reverse transcription, the PCR reaction proceeded at $95\text{ }^{\circ}\text{C}$ for 2 min, followed by 40 cycles at $95\text{ }^{\circ}\text{C}$ for 5 s and $60\text{ }^{\circ}\text{C}$ for 10 s.

After the RT-qPCR reactions, the mean cycle threshold (C_t) value of actin obtained for each sample was plotted as a function of the log of RNA concentration measured in each sample to confirm that *Actin* was constitutively expressed across all treatments and temperatures. Then, the expression of *NR* relative to the expression of *Actin* was calculated as relative transcript abundance = $2^{-(\Delta C_t)}$ (Pfaffl 2007).

Statistical analyses

Results of replicate physiological assays were averaged for each time point and then results of replicated treatments were averaged. To determine the main and interactive effects of temperature and nutrient limitation, two-way ANOVA analyses were conducted using the programming software R (R Core Team 2018) with temperature and treatment (nutrient addition) as the two independent factors. The dependent variables examined through these analyses were algal Fv/Fm, ETR_{max} , NR activity, bSiO₂ deposition (PDMPO incorporation), and relative *NR* gene expression. In addition, one-way ANOVA analyses were used to examine the effects that growth temperature and nutrient addition alone had on the physiological and gene expression measurements. Tukey's

post hoc tests were used to determine significant differences between the growth temperature and nutrient treatments.

Results

Algal growth rates and nutrient concentrations

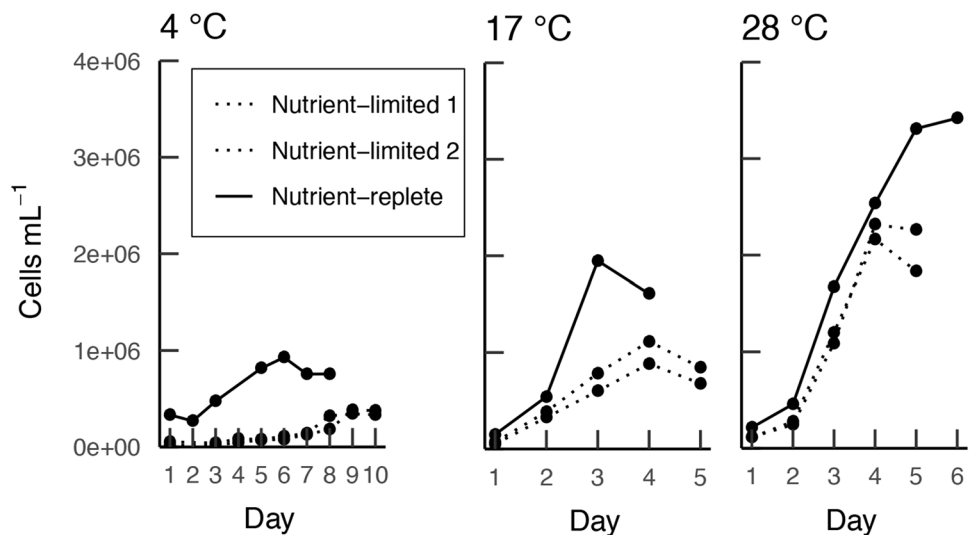
The highest growth rates were observed at $17\text{ }^{\circ}\text{C}$ and the lowest growth rates were observed at $4\text{ }^{\circ}\text{C}$ in the nutrient-replete cultures (Fig. 2). Growth rates in exponential conditions were 0.41, 1.28, and 0.66 day^{-1} for the 4, 17, and $28\text{ }^{\circ}\text{C}$ cultures, respectively. After cells were transferred to NO_3^- and Si-depleted media, the growth rates of the $28\text{ }^{\circ}\text{C}$ cultures were significantly higher than the growth rates of the 4 and $17\text{ }^{\circ}\text{C}$ cultures (one-way ANOVA/Tukey's HSD, $p < 0.01$ and $p < 0.05$, respectively), likely reflecting additional nutrient carry-over in the highest temperature transfer. Growth rates measured in the nutrient-depleted $17\text{ }^{\circ}\text{C}$ cultures were significantly higher than those of the $4\text{ }^{\circ}\text{C}$ cultures (one-way ANOVA/Tukey's HSD, $p < 0.01$). The average algal growth rates in the nutrient-depleted cultures were $0.50 \pm 0.01\text{ day}^{-1}$ at $4\text{ }^{\circ}\text{C}$, $0.91 \pm 0.01\text{ day}^{-1}$ at $17\text{ }^{\circ}\text{C}$, and $1.08 \pm 0.05\text{ day}^{-1}$ at $28\text{ }^{\circ}\text{C}$ (Fig. 2).

Immediately following nutrient enrichment, cultures that were enriched with NO_3^- had an average NO_3^- concentration of $100.4 \pm 1.63\text{ }\mu\text{M}$, while those that were not enriched with NO_3^- had an average NO_3^- concentration of $1.13 \pm 0.32\text{ }\mu\text{M}$. The cultures that were enriched with Si had an average starting Si concentration of $89.4 \pm 5.72\text{ }\mu\text{M}$ and those that did not receive Si had an average concentration of $0.99 \pm 0.18\text{ }\mu\text{M}$. After 24 h of incubation, the average concentration of NO_3^- in the NO_3^- -enriched cultures was $54.4 \pm 3.11\text{ }\mu\text{M}$ at $4\text{ }^{\circ}\text{C}$, $0.025 \pm 0.025\text{ }\mu\text{M}$ at $17\text{ }^{\circ}\text{C}$, and $6.32 \pm 1.63\text{ }\mu\text{M}$ at $28\text{ }^{\circ}\text{C}$. The concentration of Si in the Si-enriched cultures after 24 h of incubation was $38.25 \pm 2.31\text{ }\mu\text{M}$ at $4\text{ }^{\circ}\text{C}$, $38.41 \pm 11.65\text{ }\mu\text{M}$ at $17\text{ }^{\circ}\text{C}$, and $63.8 \pm 3.97\text{ }\mu\text{M}$ at $28\text{ }^{\circ}\text{C}$.

PAM analyses

The fluorometric analyses revealed that immediately following nutrient enrichment, and 24 h after nutrient enrichment, there was a significant effect of temperature on the Fv/Fm of the *T. pseudonana* cells (two-way ANOVA, $p < 0.01$ for

Fig. 2 Growth curves of nutrient-replete and nutrient-depleted *T. pseudonana* cultures. Solid lines depict the growth of the *T. pseudonana* cultures under nutrient-replete conditions and dotted lines depict the growth of the cultures under NO_3^- and Si-depleted conditions. Each line represents a true replicate that was used to calculate algal growth rates



both time points, Fig. 3). Additionally, after 24 h of incubation with nutrients, there was a significant effect of nutrient addition on Fv/Fm, as well as a significant interactive effect of nutrient addition and temperature on Fv/Fm (two-way ANOVA, $p < 0.01$ for nutrient effect and nutrient \times temperature effect). Immediately after nutrient enrichment the cultures had average Fv/Fm values of 0.37 ± 0.004 at 4 °C, 0.45 ± 0.003 at 17 °C, and 0.39 ± 0.002 at 28 °C. After 24 h of incubation with nutrients, the average Fv/Fm values of the cultures were 0.36 ± 0.006 at 4 °C, 0.44 ± 0.01 at 17 °C, and 0.37 ± 0.02 at 28 °C.

The significant effects of nutrient enrichment on algal Fv/Fm were only apparent in cultures that were grown at 4 °C and 28 °C after 24 h of incubation with nutrients (one-way ANOVA, $p < 0.01$ for both temperatures). At the 24 h time point, the control, NO_3^- , and $\text{NO}_3^- + \text{Si}$ -enriched cultures that were incubated at 4 °C had significantly higher Fv/Fm values than the cultures that were enriched with Si alone (one-way ANOVA/Tukey's HSD, $p < 0.05$,

$p < 0.05$, and $p < 0.01$, respectively). Similarly, at the 24 h time point, the Fv/Fm values were significantly higher in the 28 °C cultures that were enriched with NO_3^- and $\text{NO}_3^- + \text{Si}$ than in the cultures that were not enriched with NO_3^- (one-way ANOVA/Tukey's HSD, all relationships $p < 0.01$). In contrast, the Fv/Fm values of cultures that were grown and incubated at 17 °C were not significantly altered by nutrient enrichment.

The temperature at which the *T. pseudonana* cultures were grown had a significant effect on the ETR_{max} values measured in the cultures immediately following nutrient addition and 24 h after nutrient addition (two-way ANOVA, $p < 0.01$ for both time points, Fig. 3). At the initial time point after nutrient enrichment, the cultures had an average ETR_{max} of 25.05 ± 0.75 , 20.8 ± 0.32 , and 8.9 ± 0.42 $\mu\text{mol electrons m}^{-2} \text{s}^{-1}$ at 4, 17 and 28 °C, respectively. Then, 24 h following nutrient enrichment, the average ETR_{max} values were 23.9 ± 1.4 , 22.1 ± 2.5 , and 6.24 ± 0.54 $\mu\text{mol electrons m}^{-2} \text{s}^{-1}$ at the respective temperatures (Fig. 4).

Fig. 3 Quantum efficiency (Fv/Fm) of *T. pseudonana* immediately after, and 24 h after, nutrient-depleted cultures growing at 4, 17, and 28 °C were enriched with the nutrients indicated. Values are the average of replicated sample assays and treatments and the error bars are standard errors. Where error bars are not shown, they are too small to be depicted on the graph

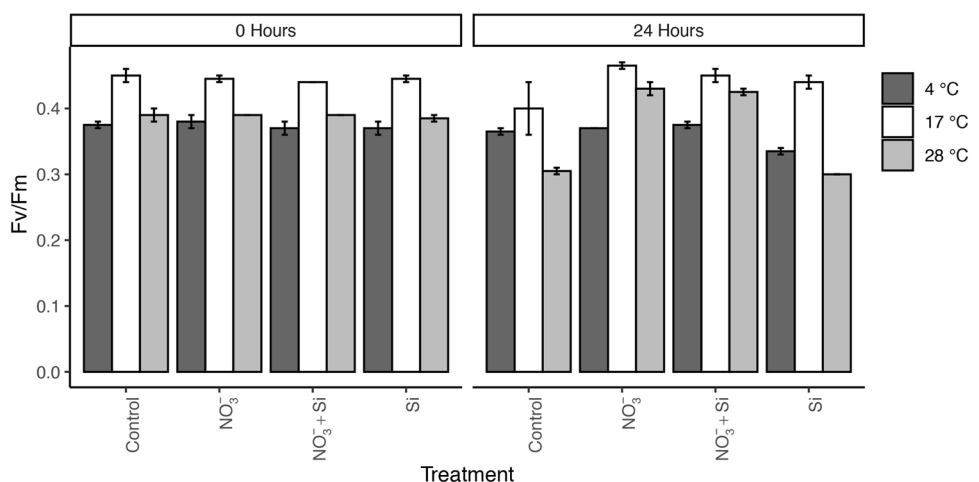
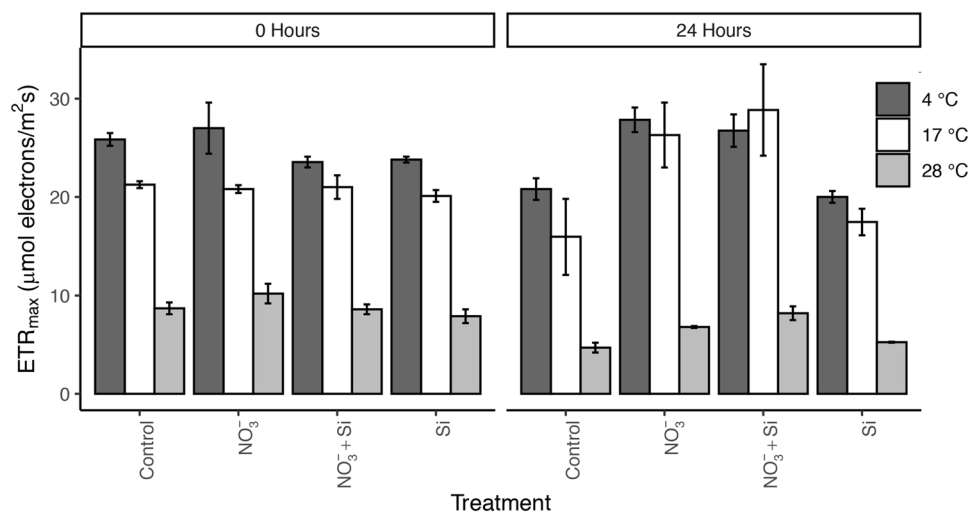


Fig. 4 Maximum electron transport rate (ETR_{max}) of *T. pseudonana* immediately after, and 24 h after, nutrient-depleted cultures growing at 4, 17, and 28 °C were enriched with the nutrients indicated. Values are the average of replicated sample assays and treatments and the error bars are standard errors. Where error bars are not shown, they are too small to be depicted on the graph



When looking at the effects of nutrient enrichment on ETR_{max} at each growth temperature, some significant trends emerged. At 4 °C, the cultures that were enriched with NO_3^- alone had a significantly higher ETR_{max} after 24 h than the control cultures or the cultures that were enriched with Si alone (one-way ANOVA/Tukey's HSD, $p < 0.05$ for both relationships). Additionally, at 28 °C, the cultures that were enriched with $\text{NO}_3^- + \text{Si}$ had a significantly higher ETR_{max} after 24 h than the control cultures and the cultures that were enriched with Si alone (one-way ANOVA/Tukey's HSD, $p < 0.05$ for both relationships). At 17 °C, nutrient enrichment did not have any significant effect on algal ETR_{max} .

NR activity analysis

Immediately following nutrient enrichment and 24 h after nutrient enrichment there was a significant effect of temperature on the activity of the NR enzyme ($p < 0.01$ for both time points, Fig. 5). The average activity of the NR enzyme was typically highest at 17 °C and lowest at 28 °C. After 24 h with nutrients, the average activity of the NR enzyme declined in all of the 17 °C *T. pseudonana* cultures. Immediately following nutrient enrichment, the average activities of the NR enzyme were 2.34 ± 0.80 , 9.57 ± 1.58 , and 2.01 ± 0.41 $\text{fmol NO}_2^- \text{ formed cell}^{-1} \text{ h}^{-1}$ at 4, 17 and 28 °C, respectively. The average activities of the NR enzyme after 24 h were 3.61 ± 0.84 , 7.54 ± 1.36 , and 2.69 ± 0.71 $\text{fmol NO}_2^- \text{ formed cell}^{-1} \text{ h}^{-1}$ at 4, 17 and 28 °C. Nutrient enrichment did not significantly affect the activity of the NR enzyme in the cultures immediately following nutrient enrichment or 24 h following nutrient enrichment (one-way ANOVA).

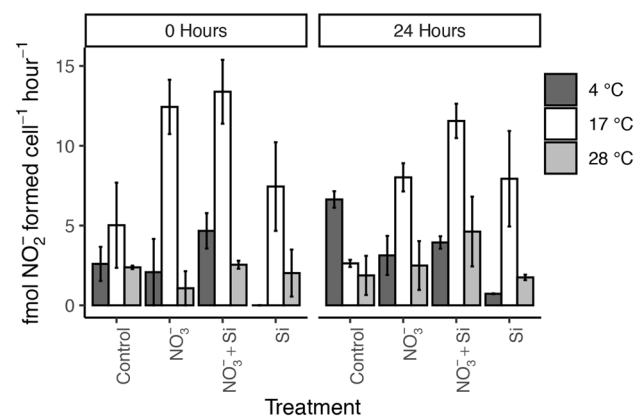


Fig. 5 Activity of nitrate reductase of *T. pseudonana* immediately after, and 24 h after, nutrient depleted cultures growing at 4, 17, and 28 °C were enriched with the nutrients indicated. Values are the average of replicated sample assays and treatments and the error bars are standard errors

PDMPO incorporation

Incorporation of PDMPO revealed that temperature and nutrient enrichment in isolation, and in combination, had a significant effect on bSiO_2 deposition immediately following nutrient enrichment (two-way ANOVA, $p < 0.01$ for nutrient enrichment, temperature, and nutrient enrichment x temperature, Fig. 6). When the cells in culture were incubated with PDMPO for 24 h after nutrient enrichment, there was a significant effect of nutrient enrichment on bSiO_2 deposition (two-way ANOVA, $p < 0.01$).

At both the initial and final time points, the cultures that were enriched with $\text{NO}_3^- + \text{Si}$ had significantly higher bSiO_2 deposition rates than rates associated with the control and NO_3^- treatments (one-way ANOVA/Tukey's HSD, $p < 0.01$ for all comparisons). When the cultures were incubated with PDMPO immediately following nutrient addition,

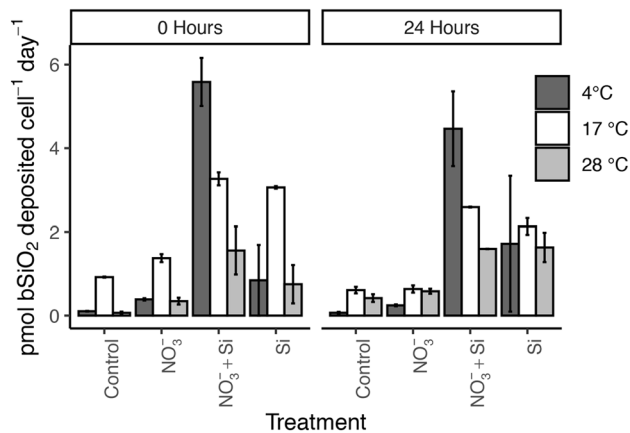


Fig. 6 The rate of bSiO₂ deposition in *T. pseudonana* immediately after, and 24 h after, nutrient-depleted cultures growing at 4, 17, and 28 °C were enriched with the nutrients indicated. Values are the average of replicated sample assays and treatments and the error bars are standard errors

the highest bSiO₂ deposition values were noted in the 4 °C NO₃⁻ + Si-enriched cultures (5.85 ± 0.58 pmol bSiO₂ cell⁻¹ h⁻¹) and the lowest bSiO₂ deposition values were observed in the 28 °C control cultures (0.065 ± 0.029 pmol bSiO₂ cell⁻¹ h⁻¹). When the cultures were incubated with PDMPO 24 h after nutrient enrichment, the highest bSiO₂ deposition values were still noted in the 4 °C NO₃⁻ + Si-enriched cultures (4.47 ± 0.90 pmol bSiO₂ cell⁻¹ h⁻¹), while the lowest bSiO₂ deposition values were noted in the 4 °C control cultures (0.069 ± 0.020 pmol bSiO₂ cell⁻¹ h⁻¹, Fig. 6).

Gene expression analyses

There was a significant effect of temperature, nutrient enrichment, and temperature x nutrient enrichment on the relative expression of the *NR* gene immediately following nutrient addition (Fig. 7). The relative expression of the *NR* gene was significantly greater in the cultures that were grown at 4 °C than in those that were grown at 17 °C (one-way ANOVA/Tukey's HSD, $p < 0.01$). The cultures that were grown at 4 °C also tended to have higher relative *NR* expression than the cultures that were grown at 28 °C, though this relationship was not statistically significant at $p < 0.05$ ($p = 0.06$). In the cultures that were grown at 4 °C, the relative expression of the *NR* gene was significantly altered by all nutrient enrichment treatments (one-way ANOVA/Tukey's HSD, $p < 0.01$ for all comparisons). In the cultures that were grown at 28 °C, the relative expression values of the cultures that were enriched with Si alone were significantly different from the control cultures at this temperature (one-way ANOVA/Tukey's HSD, $p < 0.05$).

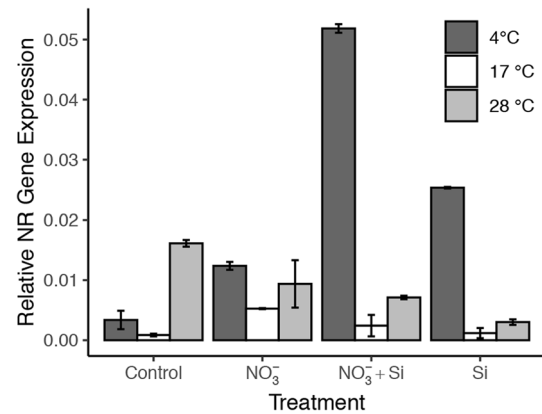


Fig. 7 Relative expression of the nitrate reductase gene in *T. pseudonana* immediately after nutrient-depleted cultures growing at 4, 17, and 28 °C were enriched with the nutrients indicated. Values are the average of replicated sample assays and treatments and the error bars are standard errors

Discussion

The overarching goal of this study was to determine how nutrient availability and water temperature synergistically impact diatom growth, photosynthetic efficiency, NR activity, and NR gene expression. The results obtained in this experiment support the hypothesis that cold, nutrient-replete conditions may lead to increases in diatom cell wall silicification. Additionally, the results of this study suggest that NR enzyme activity and NR gene expression may not be linked, and that NR enzyme activity may be regulated downstream of mRNA transcription. Lastly, this study revealed that quantum efficiency and ETR_{max} may be influenced by the growth temperature of diatom cells.

bSiO₂ deposition as a result of diatom stress response

The results of this study support the physiological mechanism outlined by Liu and Glibert (2018) that links cold water temperatures to increased silicification in at least some diatom taxa. In their proposed mechanism, Liu and Glibert (2018) suggest that under cold temperature and high-light conditions, diatom cells experience stress and may become more heavily silicified. Liu and Glibert (2018) first note that under cold temperature conditions, dissimilatory NO₃⁻ reduction may not be an effective form of photoprotection due to the fact that NR enzyme activity declines at low temperatures. They proposed that photorespiration may serve as an alternative form of photoprotection under cold temperature conditions and may promote increases in mitochondrial urea cycle activity, polyamine synthesis, and diatom cell wall silicification. The results of this study support the idea that growth at cold (~4 °C) temperatures are

stressful based on the Fv/Fm data obtained through fluorometric analyses (Fig. 3). The lower Fv/Fm values that were noted in the 4 °C cultures suggest that the cells growing at these low temperatures were stressed to some degree (Falkowski et al. 1992), though the intricate imbalances in metabolism that may have occurred at the cellular level were not accounted for in this study. Additionally, the results of this experiment suggest that NR enzyme activity may decline under cold (4 °C) temperature conditions (Fig. 5). While rates of photorespiration and urea cycle activity were not measured in this study, bSiO₂ deposition rates were measured and were influenced by both diatom growth temperature and nutrient availability (Fig. 6). Thus, bSiO₂ deposition was highest when *T. pseudonana* cells were grown and incubated at 4 °C and when cells were supplied with NO₃⁻ and Si, supporting the hypothesis that cold, nutrient-replete waters may promote silicification in diatom cells.

A number of field studies have noted increases in the abundance of heavily silicified diatom species under cold temperature, high-nutrient conditions. For example, in Sishili Bay, China, an increase in the abundance of the small, heavily silicified diatom *Paralia sulcata* during the cold winter months has been documented in recent years with increases in eutrophication and increases in N relative to Si (Liu et al. 2013; Liu and Glibert 2018). Similarly, increases in the abundance of smaller diatoms with thicker frustules have been noted in the eutrophic, Mecklenburg Bight and Arkona Sea, Baltic Sea, during the winter and early spring season and have been associated with drawdowns of NO₃⁻, phosphate (PO₄³⁻), and Si in the water column (Wasmund et al. 1998). A study conducted by Baines et al. (2010) compared diatom silicification in the cold, nutrient-replete waters of the Southern Ocean Antarctic Zone (SOAZ) to the warm, nutrient-depleted waters of the Eastern Equatorial Pacific (EEP). The results of that study revealed that diatoms living in the colder waters of the SOAZ had ~6 times more bSiO₂ per unit volume than the diatoms living in the EEP waters (Baines et al. 2010), suggesting that both nutrient availability and temperature may play a role in altering diatom cell wall thickness in these regions. Similarly, in a study conducted by Takeda (1998), Si consumption by diatoms was 2 times greater in the high-latitude waters of the Southern Ocean and the Subarctic North Pacific than they were for the low-latitude waters of the Equatorial Pacific. Together, these field observations support the notion that cold, nutrient-rich waters may lead to increased silicification in diatom cells. Importantly, separating the effects that nutrient availability and temperature have on bSiO₂ deposition in field studies remains a challenge and the effects that upwelling and NO₃⁻:Si ratios may play in influencing diatom silicification must be considered alongside any potential temperature effects.

The effects of temperature on diatom bSiO₂ deposition have also been studied in cultured algal species. A previous laboratory study conducted by Durbin (1977) found that the amount of intracellular Si per unit surface area in *Thalassiosira nordenskiöldii* was ~2 times greater in cells grown at 0 °C than in cells grown at 10 °C under nutrient-replete conditions. Similarly, in a study conducted by Paasche (1980), the Si content per diatom cell increased with decreasing temperatures (8–23 °C) in the diatoms *Chaetoceros affinis* and *Rhizosolenia fragilissima*. In a study conducted by Spilling et al. (2015), the amount of Si relative to C in Si-limited *Chaetoceros wighamii* cells was greater when cells were grown at 7 °C as opposed to 11 °C under moderate (130 μmol photons m⁻² s⁻¹) light conditions. In a more recent study conducted by Lomas et al. (2019), a number of polar diatom species were isolated and maintained under low-temperature conditions (~2 °C) to determine how these colder temperatures would affect the Si content per diatom cell as a function of cell biovolume. That study revealed that the amount of Si per diatom cell increased with cell biovolume 5–15 times more in the cells grown at cold temperatures than in diatom cells from other studies that were grown under a range of temperate conditions (Lomas et al. 2019). They further suggested that cold temperatures may increase diatom Si quotas in a similar fashion to the way in which iron limitation has been shown to increase diatom Si content. Both cold temperature conditions and iron limitation may decrease algal growth rate and cell C content without affecting Si uptake, thus leading to higher cellular Si quotas (Lomas et al. 2019). Collectively these studies do not provide a definitive mechanism to link water temperature to cell wall silicification, but instead highlight that colder temperature conditions may promote higher frustule Si content in certain diatom species and that this relationship between colder temperatures and thicker Si frustules warrants further investigation.

If environmental shifts such as temperature select for diatom cells with thicker frustules, such changes in phytoplankton ecology may, in turn, impact the overall biogeochemical cycling of Si in an aquatic ecosystem (Liu and Glibert 2018). Heavily silicified diatoms sink faster than less silicified forms and may lead to increased bSiO₂ sequestration in the sediments (Dugdale et al. 1995; Liu et al. 2013; Liu and Glibert 2018). Increased nutrient sequestration as a result of faster sinking rates can slow down the rate of bSiO₂ dissolution and may impact the subsequent availability of Si relative to other essential nutrients in the water column, especially because Si remineralization occurs at a slower rate than N, P, and C remineralization (Twining et al. 2014). Such changes in the relative availability of Si over time may promote the growth of non-silicious and potentially harmful phytoplankton species (Anderson et al. 2002; Liu and Glibert 2018).

Nitrate reductase enzyme activity and gene expression

The NR enzyme activity data and the relative expression data yield insight into NR activity and regulation in diatom cells. A previous study conducted by Vergara et al. (1998) suggested that NR activity is regulated at the transcriptional level; however, the results of this experiment do not support this idea and instead suggest that NR activity may be regulated downstream of mRNA transcription under certain environmental conditions. In this study, the relative expression of the *NR* gene was lowest at 17 °C and the activity of the NR enzyme was generally highest at 17 °C (Fig. 7), suggesting that although NR expression levels were relatively low at 17 °C, NR enzyme function remained high at this temperature. This idea of NR activity being regulated downstream of transcription may be further supported when looking at data obtained in a study conducted by Berges et al. (2002) in which NR activity analyses were performed at 3 assay temperatures using *T. pseudonana* cells isolated from 3 growth temperatures. The results of that study revealed that the temperature at which the NR assay was assessed had a greater effect on NR activity than the temperature at which the cells were grown (Berges et al. 2002). This suggests that the activity of the crude NR enzyme may be influenced by processes that occur downstream of *NR* mRNA transcription. Additionally, a transcriptomic study carried out by Bender et al. (2014) revealed that a *T. pseudonana* NR gene was upregulated in response to NO_3^- limitation, suggesting that cells may upregulate NR transcription in response to nutrient limitation. In discussing NR activity regulation, Berges et al. (2002) speculated that protease activity may alter NR protein abundance as temperatures increase. Additionally, Berges et al. (2002) commented on the potential role that post-translational modifications may play in altering the kinetic constants and the subsequent activity of the NR enzyme. Although little information about the post-translational regulation of the NR enzyme is known at this time, the findings outlined by Berges et al. (2002) and Bender et al. (2014) along with the relative *NR* expression data obtained in this study suggest that *NR* gene expression and NR activity may be decoupled and that diatoms exposed to stressful temperature conditions may upregulate NR genes to compensate for decreases in NR efficiency that occur outside of the optimal NR activity temperature range.

Changes in diatom variable fluorescence response

The growth rates of the *T. pseudonana* cells grown under nutrient-replete and nutrient-depleted conditions were highest at warmer temperatures and lowest at colder temperatures (Fig. 2). This finding is in agreement with a previous study that documented linear increases in *T. pseudonana* growth

rate when cells were grown across a broad temperature gradient (7–25 °C) under high-light, nutrient-replete conditions (Stramski et al. 2002). The similarities noted between *T. pseudonana* growth rate and temperature in this study and in the Stramski et al. (2002) study suggest that the nutrient-limited conditions that were used in this study did not alter the documented, linear relationship between temperature and *T. pseudonana* growth rate.

The fluorometric data obtained in this study suggest that moderate temperatures increase the photochemical efficiency of *T. pseudonana*. In a previous study carried out by From et al. (2014), *Chaetoceros socialis* cells that were incubated for 2 h at 5 °C had a lower Fv/Fm than cells that were incubated for 2 h at 25 °C. The authors of that study suggested that the temperature at which cells are incubated can affect the speed at which photosystems are repaired following photoinhibition (From et al. 2014). Therefore, it is possible that the *T. pseudonana* cells that were grown at 4 and 28 °C in this study had experienced some degree of photodamage as a result of temperature stress and that these temperatures impeded natural photosystem repair processes. The slowing down of these repair processes may be one explanation for the decreased algal quantum efficiency in the 4 and 28 °C cultures relative to the 17 °C cultures noted in this experiment.

The Fv/Fm data obtained in this study also revealed that nutrient availability may at times interact with temperature to influence algal quantum efficiency. It is well-known that N-limitation leads to decreases in the amount of N invested by algal cells in light-harvesting machinery, and thus may lead to decreases in the photochemical efficiency of an algal cell (Falkowski and Raven 1997). Indeed, decreases in diatom quantum efficiency under N-limitation were documented using PAM fluorometry in a study conducted by Parkhill et al. (2001). The significant increase in Fv/Fm noted in the 28 °C cultures that were enriched with NO_3^- demonstrates that these cells were able to alleviate N stress and increase quantum efficiency 24 h after nutrient enrichment (Fig. 3). In the 4 °C cultures, the control, NO_3^- , and $\text{NO}_3^- + \text{Si}$ -enriched cells had a higher Fv/Fm than the cells that were enriched with Si alone after 24 h (Fig. 3). While the higher Fv/Fm values noted in the NO_3^- , and $\text{NO}_3^- + \text{Si}$ -enriched cultures can be explained by alleviating N stress in cells, the higher Fv/Fm noted in the 4 °C control cultures relative to the 4 °C Si-enriched cultures cannot be explained by NO_3^- addition alone and requires further investigation. Importantly, the Fv/Fm values of the cultures that were grown at 17 °C did not significantly respond to nutrient enrichment, suggesting that temperature and the degree of nutrient limitation may be important in determining how algal quantum efficiency will change once nutrient stress is alleviated in diatom cells.

Herein, higher growth temperatures were associated with lower ETR_{max} values (Fig. 3). In a long-term temperature

acclimation study conducted by Mock and Hoch (2005), the polar diatom, *Fragilariopsis cylindrus*, had a higher ETR_{max} when the diatom was grown at $-1\text{ }^{\circ}\text{C}$ as opposed to $7\text{ }^{\circ}\text{C}$ (Mock and Hoch 2005). To explain the differences in ETR_{max} recorded at -1 and $7\text{ }^{\circ}\text{C}$, these authors suggested that diatoms grown at colder temperatures may absorb less light than diatoms grown at warmer temperatures, thus causing the relative ETR_{max} of the cells grown at colder temperatures to be overestimated. Much like the Mock and Hoch (2005) study, the cultures that were acclimated to colder temperature conditions in this study ($4\text{ }^{\circ}\text{C}$) had

a higher ETR_{max} , suggesting that the higher ETR_{max} may be due to differences in the amount of light absorbed by the cells at different temperatures. Importantly, the ETR_{max} values obtained with PAM fluorometry are not directly related to measurements of O_2 evolution, due to the fact that mechanisms that cells can use for energy balance, such as photorespiration, may act as electron sinks (Kromkamp et al. 1998). Therefore, it is possible that the actual ETR_{max} values of the $17\text{ }^{\circ}\text{C}$ cultures were greater than those of the $4\text{ }^{\circ}\text{C}$ cultures when considering the effects that temperature may have on light absorption and the fate of the electrons that leave photosystem II.

Conclusion

Temperature and nutrient-depleted conditions can collectively lead to imbalances in algal cellular metabolism and may, in turn, induce stress response pathways. The results of this study support the hypothesis that cold temperature conditions may stress diatom cells and increase bSiO_2 deposition in diatom frustules when nutrients are not limiting cell growth. Additionally, the results of this study suggest that NR genes may be upregulated when temperature conditions fall outside of the NR temperature optimum, thus allowing cells to compensate for a lack of NR efficiency at cold or hot temperatures by increasing the transcription of genes that are associated with the NR enzyme. These findings have implications with respect to the biogeochemical cycling of nutrients but future studies on a larger spectrum of genes, including those associated with N and Si transporters, and frustulins or silicidins would be helpful in resolving the relationship between stress and diatom bSiO_2 deposition. Even without this additional detail, the data presented in this study emphasize the importance of these physiological responses in ensuring that diatoms remain resilient under environmental stress.

Acknowledgements SJG was supported by Maryland Sea Grant under Grants # R/E-1-2018 and additional support was provided by Maryland Sea Grant R/WQ-5a and by the Cooperative Institute for the North Atlantic Region (CINAR). We thank Greg Silsbe for help with the fluorometric analyses and Sophia Ahn for help with the PAM analyses.

This is contribution number 5884 from the University of Maryland Center for Environmental Science.

Authors' contributions SJG and PMG developed and executed the study. SJG and LVP tested and confirmed gene expression analyses. SJG analyzed the data and wrote the manuscript with support from PMG and LVP. All authors contributed to the final manuscript.

Funding SJG was supported by Maryland Sea Grant under Grants # R/E-1-2018 by Maryland Sea Grant R/WQ-5a; LVP was supported by the Cooperative Institute for the North Atlantic Region (CINAR); PMG also received support from NOAA NA19NOS4780183.

Availability of data and materials The data generated from the study are contained within this manuscript. Raw data are available upon request.

Compliance with ethical standards

Conflict of interest PMG is co-owner of Bay Instruments, LLC, a distributor of Walz instruments. No other conflicts for other authors.

Ethics approval This is an observational study; no ethics approval was required.

Consent to participate Not applicable.

Consent for publication Not applicable.

References

- Anderson DM, Glibert PM, Burkholder JM (2002) Harmful algal blooms and eutrophication: nutrient sources, composition, and consequences. *Estuaries* 25:704–726. <https://doi.org/10.1007/BF02804901>
- Baines SB, Twinning BS, Brzezinski MA, Nelson DM, Fisher NS (2010) Causes and biogeochemical implications of regional differences in silicification of marine diatoms. *Glob Biogeochem Cycles* 24:1–15. <https://doi.org/10.1029/2010GB003856>
- Bender SJ, Durkin CA, Berthiaume CT, Morales RL, Armbrust EV (2014) Transcriptional responses of three model diatoms to nitrate limitation of growth. *Front Mar Sci* 1(3):1–15. <https://doi.org/10.3389/fmars.2014.00003>
- Berges JA, Harrison PJ (1995) Nitrate reductase activity quantitatively predicts the rate of nitrate incorporation under steady state light limitation: a revised assay and characterization of the enzyme in three species of marine phytoplankton. *Limnol Oceanogr* 40(1):82–93. <https://doi.org/10.4319/lo.1995.40.1.0082>
- Berges JA, Varela DE, Harrison PJ (2002) Effects of temperature on growth rate, cell composition and nitrogen metabolism in the marine diatom *Thalassiosira pseudonana* (Bacillariophyceae). *Mar Ecol Progr Ser* 225:139–146. <https://doi.org/10.3354/meps225139>
- Brzezinski MA, Villareal TA, Lipschultz F (1998) Silica production and the contribution of diatoms to new and primary production in the central North Pacific. *Mar Ecol Progr Ser* 167:89–104. <https://doi.org/10.3354/meps167089>
- Cushing DH (1989) A difference in structure between ecosystems in strong stratified waters and in those that are only weakly stratified. *J Plankt Res* 11(1):1–13. <https://doi.org/10.1093/plankt/11.1.1>
- Del Amo Y, Le Pape O, Tréguer P, Quéguiner B, Ménesguen A, Aminot A (1997) Impacts of high-nitrate freshwater inputs on

- macrotidal ecosystems. I. Seasonal evolution of nutrient limitation for the diatom-dominated phytoplankton of the Bay of Brest (France). *Mar Ecol Progr Ser* 161:213–224. <https://doi.org/10.3354/meps161213>
- Doane TA, Horwath WR (2003) Spectrophotometric determination of nitrate with a single reagent. *Anal Lett* 36(12):2713–2722. <https://doi.org/10.1081/AL-120024647>
- Dugdale RC, Wilkerson FP, Minas HJ (1995) The role of a silicate pump in driving new production. *Deep Sea Res Part I* 42(5):697–719. [https://doi.org/10.1016/0967-0637\(95\)00015-X](https://doi.org/10.1016/0967-0637(95)00015-X)
- Durbin EG (1977) Studies on the autoecology of the marine diatom *Thalassiosira nordenskiöldii*. II. The influence of cell size on growth rate, and carbon, nitrogen, chlorophyll a and silica content. *J Phycol* 13(2):150–155. <https://doi.org/10.1111/j.1529-8817.1977.tb02904.x>
- Eppley RW, Coatsworth JL, Solórzano L (1969a) Studies of nitrate reductase in marine phytoplankton. *Limnol Oceanogr* 14(2):194–205. <https://doi.org/10.4319/lo.1969.14.2.0194>
- Eppley RW, Rogers JN, McCarthy JJ (1969b) Half-saturation constants for uptake of nitrate and ammonium by marine phytoplankton. *Limnol Oceanogr* 14(6):912–920. <https://doi.org/10.4319/lo.1969.14.6.0912>
- Falkowski PG, Raven JA (1997) Aquatic photosynthesis. Blackwell Science, Malden, p 375
- Falkowski PG, Greene RM, Geider RJ (1992) Physiological limitations on phytoplankton productivity in the ocean. *Oceanography* 5(2):84–91. <https://doi.org/10.5670/oceanog.1992.14>
- Finlay BJ, Fenchel T (2004) Cosmopolitan metapopulations of free-living microbial eukaryotes. *Protist* 155:237–244. <https://doi.org/10.1078/143446104774199619>
- From N, Richardson K, Mousing EA, Jensen PE (2014) Removing the light history signal from normalized variable fluorescence (F/F) measurements on marine phytoplankton. *Limnol Oceanogr Methods* 12(11):776–783
- Gao Y, Smith GJ, Alberte RS (2000) Temperature dependence of nitrate reductase activity in marine phytoplankton: biochemical analysis and ecological implications. *J Phycol* 36:304–313. <https://doi.org/10.1046/j.1529-8817.2000.99195.x>
- Genty B, Briantais JM, Baker NR (1989) The relationship between the quantum yield of photosynthetic electron transport and quenching of chlorophyll fluorescence. *BBA Gen Subj* 990:87–92. [https://doi.org/10.1016/S0304-4165\(89\)80016-9](https://doi.org/10.1016/S0304-4165(89)80016-9)
- Glibert PM, Wilkerson FP, Dugdale RC, Raven JA, Dupont CL, Leavitt PR, Parker AE, Burkholder JM, Kana TM (2016) Pluses and minuses of ammonium and nitrate uptake and assimilation by phytoplankton and implications for productivity and community composition, with emphasis on nitrogen-enriched conditions. *Limnol Oceanogr* 61:165–197. <https://doi.org/10.1002/lno.10203>
- Goldman JC (1993) Potential role of large oceanic diatoms in new primary production. *Deep Sea Res Part I* 40(1):159–168. [https://doi.org/10.1016/0967-0637\(93\)90059-C](https://doi.org/10.1016/0967-0637(93)90059-C)
- Granum E, Raven JA, Leegood RC (2005) How do marine diatoms fix 10 billion tonnes of inorganic carbon per year? *Can J Bot* 83:898–908. <https://doi.org/10.1139/b05-077>
- Guillard RRL (1983) Culture of phytoplankton for feeding marine invertebrates. In: Berg CO Jr (ed) Culture of marine invertebrates: selected readings. Hutchinson Ross Publishing, Stroudsberg, pp 108–132
- Hildebrand M, Lerch SJ, Shrestha RP (2018) Understanding diatom cell wall silicification—moving forward. *Front Mar Sci* 5:125. <https://doi.org/10.3389/fmars.2018.00125>
- Huner NPA, Öquist G, Sarhan F (1998) Energy balance and acclimation to light and cold. *Trends Plant Sci* 3(6):224–230. [https://doi.org/10.1016/S1360-1385\(98\)01248-5](https://doi.org/10.1016/S1360-1385(98)01248-5)
- Kok B (1956) On the inhibition of photosynthesis by intense light. *Biochim Biophys Acta* 21(2):234–244. [https://doi.org/10.1016/0006-3002\(56\)90003-8](https://doi.org/10.1016/0006-3002(56)90003-8)
- Kromkamp J, Barranguet C, Peene J (1998) Determination of microphytobenthos PSII quantum efficiency and photosynthetic activity by means of variable chlorophyll fluorescence. *Marine Ecol Progr Ser* 162:45–55
- Kristiansen S (1983) The temperature optimum of the nitrate reductase assay for marine phytoplankton. *Limnol Oceanogr* 28(4):776–780. <https://doi.org/10.4319/lo.1983.28.4.0776>
- Li WKW (1980) Temperature adaptation in phytoplankton: cellular and photosynthetic characteristics. In: Falkowski PG (ed) Primary productivity in the sea. Plenum Press, New York, pp 259–279
- Liu D, Glibert PM (2018) Ecophysiological linkage of nitrogen enrichment to heavily silicified diatoms in winter. *Mar Ecol Progr Ser* 604:51–63. <https://doi.org/10.3354/meps12747>
- Liu D, Shen DX, Di B, Shi Y, Keesing JK, Wang Y, Wang Y (2013) Palaeoecological analysis of phytoplankton regime shifts in response to coastal eutrophication. *Mar Ecol Progr Ser* 475:1–14. <https://doi.org/10.3354/meps10234>
- Lomas MW, Glibert PM (1999a) Temperature regulation of nitrate uptake: a novel hypothesis about nitrate uptake and reduction in cool-water diatoms. *Limnol Oceanogr* 44(3):556–572. <https://doi.org/10.4319/lo.1999.44.3.0556>
- Lomas MW, Glibert PM (1999b) Interactions between NH_4^+ and NO_3^- uptake and assimilation: comparison of diatoms and dinoflagellates at several growth temperatures. *J Phycol* 36:903–913. <https://doi.org/10.1007/s002270050494>
- Lomas MW, Baer SE, Acton S, Krause JW (2019) Pumped up by the cold: elemental quotas and stoichiometry of cold-water diatoms. *Front Mar Sci* 6:286. <https://doi.org/10.3389/fmars.2019.00286>
- McGinn PJ, Morel FMM (2008) Expression and regulation of carbonic anhydrases in the marine diatom *Thalassiosira pseudonana* and in natural phytoplankton assemblages from Great Bay, New Jersey. *Physiol Plant* 133(1):78–91. <https://doi.org/10.1111/j.1399-3054.2007.01039.x>
- McNair HM, Brzezinski MA, Krause JW (2015) Quantifying diatom silicification with the fluorescent dye, PDMPO. *Limnol Oceanogr Methods* 13(10):587–599. <https://doi.org/10.1002/lom3.10049>
- Miranda KM, Espey MG, Wink DA (2001) A rapid, simple spectrophotometric method for simultaneous detection of nitrate and nitrite. *Nitric Oxide* 5(1):62–71. <https://doi.org/10.1006/niox.2000.0319>
- Mock T, Hoch N (2005) Long-term temperature acclimation of photosynthesis in steady-state cultures of the polar diatom *Fragilariopsis cylindrus*. *Photosyn Res* 85:307–317. <https://doi.org/10.1007/s11120-005-5668-9>
- Nunn BL, Faux JF, Hippmann AA, Maldonado MT, Harvey RT, Goodlett DR, Boyd PW, Strzepak RF (2013) Diatom proteomics reveals unique acclimation strategies to mitigate Fe limitation. *PLoS ONE* 8:e75653. <https://doi.org/10.1371/journal.pone.0075653>
- Paasche E (1980) Silicon content of five marine phytoplankton diatom species measured with a rapid filter method. *Limnol Oceanogr* 25(3):474–480. <https://doi.org/10.4319/lo.1980.25.3.0474>
- Parker MS, Armbrust EV (2005) Synergistic effects of lights, temperature, and nitrogen source on transcription of genes for carbon and nitrogen metabolism in the centric diatom *Thalassiosira pseudonana* (Bacillariophyceae). *J Phycol* 41(6):1142–1153. <https://doi.org/10.1111/j.1529-8817.2005.00139.x>
- Parkhill JP, Maillet G, Cullen JJ (2001) Fluorescence-based maximal quantum yield for PSII as a diagnostic of nutrient stress. *J Phycol* 37:517–529. <https://doi.org/10.1046/j.1529-8817.2001.03700.4517.x>
- Parsons TR, Maita Y, Lalli CM (1984) A manual of chemical and biological methods for seawater analyses. Pergamon Press, New York, p 173

- Peinert R, von Bodungen B, Smetacek VS (1989) Food web structure and loss rate. In: Berger WH, Smetacek VS, Wefer G (eds) Productivity of the ocean: present and past. Wiley, Berlin, pp 53–68
- Pfaffl MW (2007) Relative quantification. In: Dorak MT (ed) Real-time PCR. Taylor & Francis, New York, pp 89–108
- Probyn TA, Painting SJ (1985) Nitrogen uptake by size-fractionated phytoplankton populations in Antarctic surface waters. *Limnol Oceanogr* 30(6):1327–1332. <https://doi.org/10.4319/lo.1985.30.6.1327>
- R Core Team (2018) R: a language and environment for statistical computing. R Foundation for Statistical Computing, Vienna
- Ragueneau O, Schultes S, Bidle K, Claquin P, Moriceau B (2006) Si and C interactions in the world ocean: importance of ecological processes and implications for the role of diatoms in the biological pump. *Glob Biogeochem Cycles* 20(4):GB4S02. <https://doi.org/10.1029/2006gb002688>
- Ras M, Steyer JP, Bernard O (2013) Temperature effect on microalgae: a crucial factor for outdoor production. *Rev Environ Sci Bio/Technol* 12(2):153–164. <https://doi.org/10.1007/s11157-013-9310-6>
- Raven JA, Falkowski PG (1999) Oceanic sinks for atmospheric CO₂. *Plant Cell Environ* 22:741–755. <https://doi.org/10.1046/j.1365-3040.1999.00419.x>
- Round FE, Crawford RM, Mann DG (1990) Diatoms: biology and morphology of the genera. Cambridge University Press, Cambridge, p 747
- Shimizu K, Del Amo Y, Brzezinski MA, Stucky GD, Morse DE (2001) A novel fluorescent silica tracer for biological silicification studies. *Chem Biol* 8:1051–1060. [https://doi.org/10.1016/S1074-5521\(01\)00072-2](https://doi.org/10.1016/S1074-5521(01)00072-2)
- Smetacek V (1998) Diatoms and the silicate factor. *Nature* 391:224–225. <https://doi.org/10.1038/34528>
- Smith JC, Platt T (1985) Temperature responses of ribulose biphosphate carboxylase and photosynthetic capacity in arctic and tropical phytoplankton. *Mar Ecol Progr Ser* 25:31–37. <https://doi.org/10.3354/meps025031>
- Sobrinho C, Neale PJ (2007) Short-term and long-term effects of temperature on photosynthesis in the diatom *Thalassiosira pseudonana* under UVR exposures. *J Phycol* 43:426–436. <https://doi.org/10.1111/j.1529-8817.2007.00344.x>
- Spilling K, Ylöstalo P, Simis S, Seppälä J (2015) Interaction effects of light, temperature and nutrient limitations (N, P and Si) on growth, stoichiometry and photosynthetic parameters of the cold-water diatom *Chaetoceros wighamii*. *PLoS ONE* 10(5):e0126308. <https://doi.org/10.1371/journal.pone.0126308>
- Stramski D, Sciandra A, Claustre H (2002) Effects of temperature, nitrogen, and light limitation on the optical properties of the marine diatom *Thalassiosira pseudonana*. *Limnol Oceanogr* 47(2):392–403. <https://doi.org/10.4319/lo.2002.47.2.0392>
- Sumper M, Kröger N (2004) Silica formation in diatoms: the function of long-chain polyamines and silaffins. *J Mater Chem* 14:2059–2065. <https://doi.org/10.1039/B401028K>
- Takeda S (1998) Influence of iron availability of nutrient consumption ratio of diatoms in oceanic waters. *Nature* 393(6687):744. <https://doi.org/10.1038/31674>
- Twinning BS, Nodder SD, King AL, Hutchins DA, LeClerc GR, DeBruyn JM, Maas EW, Vogt S, Wilhelm SW, Boyd PW (2014) Differential remineralization of major and trace elements in sinking diatoms. *Limnol Oceanogr* 59(3):689–704. <https://doi.org/10.4319/lo.2014.59.3.0689>
- Vergara JJ, Berges JA, Falkowski PG (1998) Diel periodicity of nitrate reductase activity and protein levels in the marine diatom *Thalassiosira weissflogii* (Bacillariophyceae). *J Phycol* 34:952–961. <https://doi.org/10.1046/j.1529-8817.1998.340952.x>
- Wacker MJ, Godard MP (2005) Analysis of one-step and two-step real-time RT-PCR using SuperScript III. *J Biomol Techn* 16:266–271
- Wasmund N, Nausch G, Matthäus W (1998) Phytoplankton spring blooms in the Southern Baltic Sea—spatio-temporal development and long-term trends. *J Plankt Res* 20:1099–1117. <https://doi.org/10.1093/plankt/20.6.1099>
- Zimmerman C, Price M, Montgomery J (1977) Operation, methods and quality control of Technicon AutoAnalyzer II systems for nutrient determination in seawater. Harbor Branch Foundation, Inc., Technical Report No. 11. Harbor Branch Foundation, Inc., Fort Pierce, Florida

Publisher's Note Springer Nature remains neutral with regard to jurisdictional claims in published maps and institutional affiliations.